The Role of Oxoammonium Cation in the SOD-Mimic Activity of Cyclic Nitroxides

Sara Goldstein,*,[†] Gabor Merenyi,[§] Angelo Russo,[‖] and Amram Samuni[‡]

Contribution from the Department of Physical Chemistry, The Hebrew University of Jerusalem, Jerusalem 91904, Israel, Department of Molecular Biology, The Hebrew University of Jerusalem - Hadassah Medical School, Jerusalem 91120, Israel, Department of Chemistry, Nuclear Chemistry, The Royal Institute of Technology, S-10044 Stockholm 70, Sweden, and Radiation Biology Branch, National Cancer Institute, National Institutes of Health, Bethesda, Maryland 20892, USA

Received August 18, 2002 ; E-mail: sarag@vms.huji.ac.il

Abstract: Cyclic nitroxides (RNO$^\bullet$) mimic the activity of superoxide dismutase (SOD) and demonstrate antioxidant properties in numerous in vitro and in vivo models. Their broad antioxidant activity may involve the participation of their reduced and oxidized forms, that is, hydroxylamine (RNO-H) and oxoammonium cation (RNO$^+$). To examine this possibility we studied the reactions of RNO$^\bullet$ and RNO$^+$ with HO$_2^\bullet$/O$_2^{\bullet-}$ and with several reductants by pulse radiolysis and rapid-mixing stopped-flow techniques. The oxoammonium cations were generated by electrochemical and radiolytic oxidation of 2,2,6,6-tetramethylpiperidinoxyl (TPO) and 3-carbamoyl-2,2,5,5-tetramethylpyrrolidinoxyl (3-CP). The rate constant for the reaction of RNO$^\bullet$ with HO$_2^\bullet$ to form RNO$^+$ was determined to be $(1.2 \pm 0.1) \times 10^8$ for TPO and $(1.3 \pm 0.1) \times 10^6$ M^{-1} s^{-1} for 3-CP. The kinetics results demonstrate that the reaction of RNO$^\bullet$ with HO$_2^\bullet$ proceeds via an inner-sphere electron-transfer mechanism. The rate constant for the reaction of RNO$^\bullet$ with O$_2^{\bullet-}$ is lower than 1×10^3 M^{-1} s^{-1}. The rate constant for the reaction of RNO$^+$ with O$_2^{\bullet-}$ was determined to be $(3.4 \pm 0.2) \times 10^9$ for TPO$^+$ and $(5.0 \pm 0.2) \times 10^9$ M^{-1} s^{-1} for 3-CP$^+$. Hence, both nitroxides catalyze the dismutation of superoxide through the RNO$^\bullet$/RNO$^+$ redox couple, and the dependence of the catalytic rate constant, k_{cat}, on pH displayed a bell-shaped curve having a maximum around pH 4. The oxoammonium cation oxidized ferrocyanide and HO$_2^-$ by a one-electron transfer, whereas the oxidation of methanol, formate, and NADH proceeded through a two-electron-transfer reaction. The redox potential of RNO$^\bullet$/RNO$^+$ couple was calculated to be 0.75 and 0.89 V for 3-CP and TPO, respectively. The elucidated mechanism provides a clearer insight into the biological antioxidant properties of cyclic nitroxides that should permit design of even more effective antioxidants.

Introduction

The observation that several cyclic nitroxides, including oxazolidine, piperidine, and pyrrolidine derivatives catalyze the removal of superoxide (HO$_2^\bullet$/O$_2^{\bullet-}$) prompted many studies of their antioxidative activity. These studies showed that nitroxides attenuate oxidative damage in various experimental models such as cells,[1-4] hyperoxia-induced brain damage,[5] experimental pancreatitis,[6] lipid peroxidation in liver microsomes,[7] thymocyte apoptosis,[8] xenobiotics toxicity,[9] intestinal and gastric lesions,[10] and closed-head injury induced by mechanical trauma.[11] Since nitroxides have shown such varied and beneficial effects, a better understanding of the mechanism underlying their antioxidative activity will improve and extend their use.

Nitroxides undergo one-electron redox reactions to yield the respective hydroxylamine and oxoammonium cation, as shown below for 2,2,6,6,-tetramethylpiperidinoxyl (TPO).

$$\text{(1)}$$
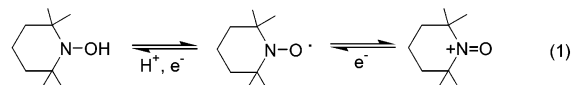
The ability of nitroxide to catalyze superoxide dismutation has been previously demonstrated by the persistence of its

[†] The Hebrew University of Jerusalem.
[‡] The Hebrew University of Jerusalem - Hadassah Medical School.
[§] The Royal Institute of Technology.
[‖] National Cancer Institute, National Institutes of Health.

(1) Mitchell, J. B.; Samuni, A.; Krishna, M. C.; DeGraff, W. G.; Ahn, M. S.; Samuni, U.; Russo, A. *Biochemistry* **1990**, *29*, 2802–2807.
(2) Samuni, A.; Winkelsberg, D.; Pinson, A.; Hahn, S. M.; Mitchell, J. B.; Russo, A. *J. Clin. Invest.* **1991**, *87*, 1526–1530.
(3) Reddan, J. R.; Sevilla, M. D.; Giblin, F. J.; Padgaonkar, V.; Dziedzic, D. C.; Leverenz, V.; Misra, I. C.; Peters, J. L. *Exp. Eye Res.* **1993**, *56*, 543–554.
(4) Krishna, M. C.; Samuni, A. *Methods Enzymol.* **1994**, *234*, 580–589.
(5) Howard, B. J.; Yatin, S.; Hensley, K.; Allen, K. L.; Kelly, J. P.; Carney, J.; Butterfield, D. A. *J. Neurochem.* **1996**, *67*, 2045–2050.
(6) Sledzinski, Z.; Wozniak, M.; Antosiewicz, J.; Lezoche, E.; Familiari, M.; Bertoli, E.; Greci, L.; Brunelli, A.; Mazera, N.; Wajda, Z. *Int. J. Pancreatol.* **1995**, *18*, 153–160.

(7) Miura, Y.; Utsumi, H.; Hamada, A. *Arch. Biochem. Biophys*. **1993**, *300*, 148–156.
(8) Slater, A. F.; Nobel, C. S.; Maellaro, E.; Bustamante, J.; Kimland, M.; Orrenius, S. *Biochem. J.* **1995**, *306*, 771–778.
(9) Konovalova, N. P.; Diatchkovskaya, R. F.; Volkova, L. M.; Varfolomeev, V. N. *Anticancer Drugs* **1991**, *2*, 591–595.
(10) Rachmilewitz, D.; Karmeli, F.; Okon, E.; Samuni, A. *Gut* **1994**, *35*, 1181–1188.
(11) Beit-Yannai, E.; Zhang, R.; Trembovler, V.; Samuni, A.; Shohami, E. *Brain Res.* **1996**, *717*, 22–28.

concentration under a flux of superoxide. Initially, Finkelstein et al.[12] reported that superoxide progressively reduces nitroxides, such as TPO, only in the presence of thiols. They proposed an equilibrium reaction, in which superoxide reversibly adds to the aminoxyl moiety of the nitroxide, forming an intermediate adduct that is reducible by thiols.[12] On the other hand, the failure of superoxide to affect the concentration of piperidine nitroxide derivatives in the absence of thiols led to an erroneous conclusion that such nitroxides do not react with superoxide at all.[13] Later, it was realized that piperidine nitroxides in the absence of reductants in fact do remove superoxide in a catalytic fashion mimicking that of SOD.[14] The reduction of the nitroxide to the hydroxylamine by superoxide in the presence of NADH,[15] and the decrease of the catalytic activity upon increasing the pH,[16] suggested the formation of the oxoammonium cation as an intermediate (reactions 2−3):[15,16]

$$RNO^{\bullet} + HO_2^{\bullet} \rightarrow RNO^+ + HO_2^- \qquad (2)$$

$$RNO^+ + O_2^{\bullet-} \rightarrow RNO^{\bullet} + O_2 \qquad (3)$$

This mechanism was further supported by a report of an indirect determination of $k_3 = 1.5 \times 10^{10} \ M^{-1} \ s^{-1}$ for TPO,[17] which is one of the highest rate constants of reactions ever reported for $O_2^{\bullet-}$.

In the present work the oxoammonium cations were prepared electrochemically as previously described[18] and radiolytically from TPO and 3-carbamoyl-proxyl (3-CP), and their reactions with various substrates including superoxide were studied.

Experimental Section

Materials and Methods. All chemicals were of analytical grade and were used as received. The nitroxides TPO and 3-CP were purchased from Aldrich. Reduced β-nicotinamide adenine dinucleotide (NADH) grade III from yeast was obtained from Sigma. The concentration of NADH was determined spectrophotometrically using $\epsilon_{340} = 6200$ $M^{-1} \ cm^{-1}$. Sodium iodide, potassium ferrocyanide, and 2,2′-azino-bis(3-ethylbenzothiazoline-6-sulfonate) (ABTS^{2-}) were purchased from Sigma, and their fresh solutions were prepared daily. Tetranitromethane (TNM) was purchased from Aldrich, dissolved in ethanol, and diluted in water. The concentration of H_2O_2 was determined spectrophotometrically following oxidation of ferrous ions in 0.8 N H_2SO_4 and using $\epsilon_{302}(Fe^{3+}) = 2197 \ M^{-1} \ cm^{-1}$. Solutions were prepared with deionized water that was distilled and purified using a Milli-Q water purification system. The oxoammonium cations were prepared in aerated solutions using an electrochemical reactor, similar to that previously described.[19] The cell consisted of a working electrode of graphite grains packed inside a porous Vycor glass tube (5 mm i.d.), through which the nitroxide solutions in 4 mM phosphate buffer (PB) at pH 7.0 were pumped (2−5 mL min^{-1}). An outer glass cylinder, with separate electrolyte (10 mM PB, pH 7.0) contained the platinum auxiliary electrode. The voltage was controlled by a homemade power supply.

(12) Finkelstein, E.; Rosen, G. M.; Rauckman, E. J. *Biochim. Biophys. Acta* **1984**, *802*, 90−98.
(13) Samuni, A.; Min, A.; Krishna, C. M.; Mitchell, J. B.; Russo, A. *Adv. Exp. Med. Biol* **1990**, *264*, 85−92.
(14) Samuni, A.; Krishna, C. M.; Mitchell, J. B.; Collins, C. R.; Russo, A. *Free Radical Res. Commun.* **1990**, , 241−249.
(15) Krishna, M. C.; Grahame, D. A.; Samuni, A.; Mitchell, J. B.; Russo, A. *Proc. Natl. Acad. Sci. U.S.A.* **1992**, *89*, 5537−5541.
(16) Krishna, M. C.; Russo, A.; Mitchell, J. B.; Goldstein, S.; Dafni, H.; Samuni, A. *J. Biol. Chem.* **1996**, *271*, 26026−26031.
(17) Vorob'eva, T. P.; Durova, R. L.; Kozlov, Y. N.; Petrov, A. N.; Pourmal, A. P. *Zh. Fiz. Khim.* **1986**, *60*, 598−602.
(18) Fish, J. R.; Swarts, S. G.; Sevilla, M. D.; Malinski, T. *J. Phys. Chem.* **1988**, *92*, 3745−3751.
(19) Miner, D. J.; Kissinger, P. T. *Biochem. Pharmacol.* **1979**, *28*, 3285−3290.
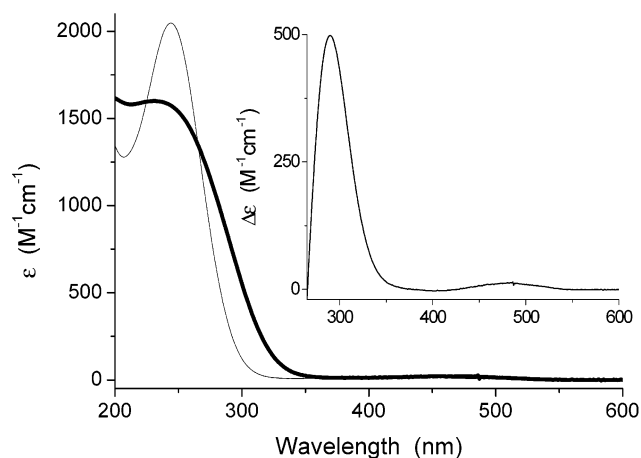
Figure 1. Respective spectra of 185 μM TPO in 4 mM PB at pH 7.0 before and after (bold) electrooxidation. (Inset) Differential spectrum having maximum absorption at 290 and 486 nm.

Immediately following electrooxidation the solution was pumped through a 1-cm optical flow cell positioned within a Hewlett-Packard 8453 diode array spectrophotometer. The oxoammonium cations thus produced were stable for 2−3 h. This allowed the study of their reactions using rapid-mixing stopped-flow, oximetry, and pulse radiolysis techniques. The oxoammonium cations rapidly oxidized Fe(CN)$_6^{4-}$. The reaction was too fast to be followed using the stopped-flow technique, but the measured yield of Fe(CN)$_6^{3-}$ ($\epsilon_{420} = 1000 \ M^{-1} \ cm^{-1}$) was used to determine the concentration of the oxoammonium cation formed electrochemically.

The yield of oxygen formed through the oxidation of H_2O_2 by the oxoammonium cation was determined by using a Clark electrode oximetry. Briefly, the oximeter was calibrated using anoxic, air-saturated and O_2-saturated solutions at 25 °C and 690 mmHg. The cell was filled (1.8 mL) with aerated solutions of 180−360 μM oxoammonium cation in 4 mM PB at pH 7.0. After temperature equilibration (25 °C), 20 μL of 30% H_2O_2 was injected into the oximeter cell through the stopper, and the increase in dioxygen concentration was determined.

Rapid-mixing stopped-flow kinetic measurements were carried out using the Bio SX-17MV Sequential Stopped-Flow from Applied Photophysics with a 1-cm optical path. Solutions of electrochemically prepared oxoammonium cation in 4 mM PB (pH 7.0) were mixed with various solutions in a 1:1 ratio. The final pH in each experiment was measured at the outlet of the stopped-flow system. All experiments were carried out at 25 °C. Pulse radiolysis experiments were carried out with a Varian 7715 linear accelerator with 5 MeV electron pulses of 0.1−1.5 μs duration. A 200-W xenon lamp produced the analyzing light. Appropriate cutoff filters were used to minimize photochemistry. All measurements were made at room temperature in a 4 cm Spectrosil cell using three light passes (optical path length 12.1 cm). The irradiation dose was 3.2−34 Gy per pulse as determined by the thiocyanate dosimetry in N_2O-saturated water.

Modeling of the experimental results was carried out using INTKIN, a noncommercial program developed at Brookhaven National Laboratories by Dr. H. A. Schwarz.

Results

TPO$^+$ and 3-CP$^+$ were formed electrochemically in aerated solutions at pH 7.0, and their yields exceeded 92%. The respective spectra of the nitroxide and its oxidized form are given in Figures 1 and 2. The differential spectra are presented in the inset of these figures and demonstrate that the decay of the oxoammonium cations can be readily followed spectrophotometrically at 270−320 nm. These oxoammonium cations rapidly oxidized ferrocyanide ($\epsilon_{420} = 1000 \ M^{-1} \ cm^{-1}$), 0.1 M
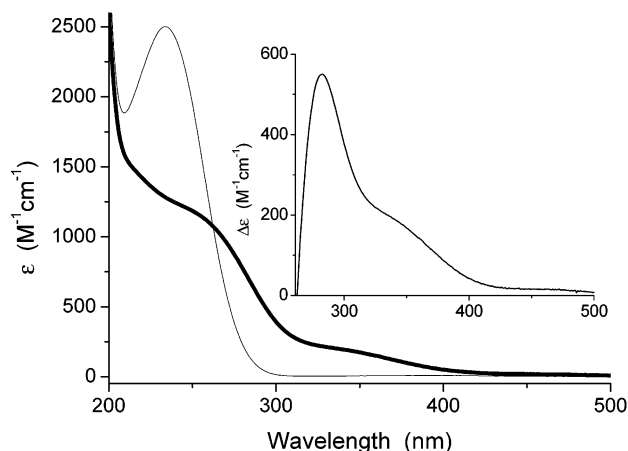
Figure 2. Respective spectra of 200 μM 3-CP in 4 mM PB at pH 7.0 before and after (bold) electrooxidation. (Inset) Differential spectrum having maximum absorption at 282 nm.
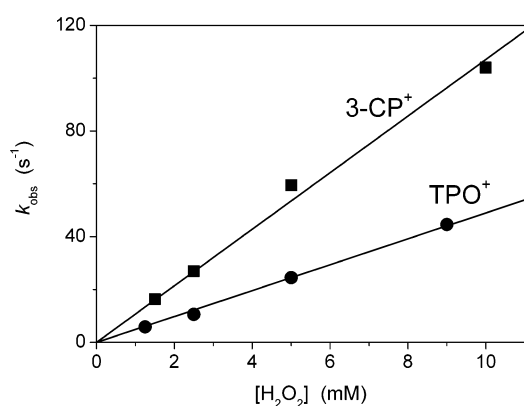

Figure 3. Reaction of H_2O_2 with oxoammonium cations. H_2O_2 in 40 mM PB was equally mixed with 180 μM TPO+ (●) or 300 μM 3-CP+ (■) in 4 mM PB. The final pH was 6.9.

Table 1. Observed Bimolecular Rate Constant (M^{-1} s^{-1}) for the Reaction of the Oxoammonium Cation with H_2O_2 as a Function of pH

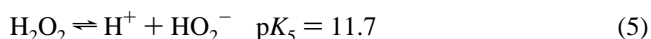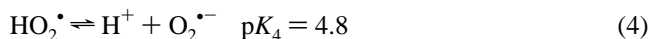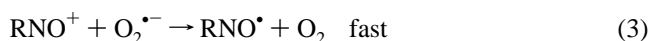| pH	TPO+	3-CP+
4.0	5.1 ± 0.1	
5.6	$(2.3 \pm 0.1) \times 10^2$	$(5.0 \pm 0.2) \times 10^2$
6.9	$(4.9 \pm 0.1) \times 10^3$	$(1.1 \pm 0.1) \times 10^4$
8.0	$(5.0 \pm 0.3) \times 10^4$	$(1.3 \pm 0.2) \times 10^5$

iodide ($\epsilon_{352}(I_3^-) = 25800$ M^{-1} cm^{-1}) and ABTS^{2-} (ϵ_{660}(ABTS$^{\bullet-}$) = 12000 M^{-1} cm^{-1}). The yields of ferricyanide and I_3^- were similar; however, that of ABTS$^{\bullet-}$ was somewhat lower, suggesting the formation of some nonabsorbing species as in the reaction of $^{\bullet}$OH with ABTS^{2-}.[20]

The Reaction of the Oxoammonium Cation with H_2O_2. The kinetics of the reaction of TPO+ and 3-CP+ with excess H_2O_2 were studied by following the decrease of the absorption at 282 and 300 nm, respectively. The decay of the oxoammonium cation obeyed first-order kinetics, and k_{obs} was linearly dependent on $[H_2O_2]$ (Figure 3) and increased upon increasing the pH from 5.6 to 8.0 (Table 1). The reaction at pH > 8 was too fast for a kinetic study using this technique. The yield of O_2 formed upon the reaction of the oxoammonium cation with H_2O_2 was determined oximetrically at pH 7.0 to be $50 \pm 5\%$,

(20) Wolfenden, B. S.; Willson, R. L. *J. Chem. Soc., Perkin Trans. 2* **1982**, 805−812.
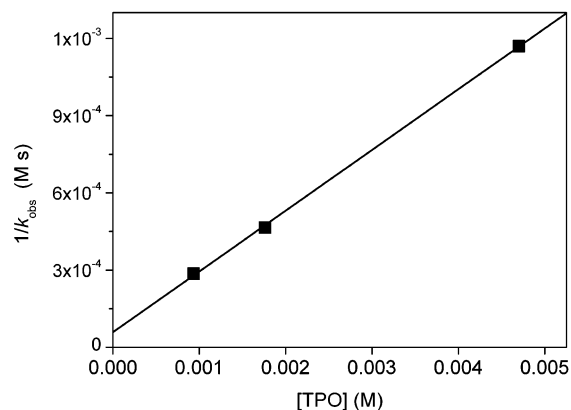
Figure 4. Reaction of TPO+ with H_2O_2 in the presence of added TPO. TPO+ (180 μM) in 4 mM PB at pH 7.0 was equally mixed 0.18 M H_2O_2 in 0.1 M acetate buffer at pH 4.0 containing 1.86−9.4 mM TPO. The final pH was 4.0.

that is, $\Delta[O_2]/\Delta[RNO^+] = 0.50 \pm 0.05$. This suggests that the oxidation of H_2O_2 takes place via a one-electron-transfer mechanism:

$$RNO^+ + HO_2^- \rightleftharpoons RNO^{\bullet} + HO_2^{\bullet} \qquad (-2)$$

$$RNO^+ + O_2^{\bullet-} \rightarrow RNO^{\bullet} + O_2 \quad \text{fast} \qquad (3)$$

$$HO_2^{\bullet} \rightleftharpoons H^+ + O_2^{\bullet-} \quad pK_4 = 4.8 \qquad (4)$$

$$H_2O_2 \rightleftharpoons H^+ + HO_2^- \quad pK_5 = 11.7 \qquad (5)$$

Assuming the steady-state approximation for superoxide, rate eq 6 is obtained at pH $\ll$ pK_5:

$$-\frac{d[RNO^+]}{dt} = \frac{2k_{-2}k_3(K_4/[H^+])(K_5/[H^+])[H_2O_2]_o[RNO^+]^2}{k_2[RNO^{\bullet}] + k_3(K_4/[H^+])[RNO^+]} \qquad (6)$$

Without the addition of RNO$^{\bullet}$, $k_2[RNO^{\bullet}]$ remains much less than $k_3(K_4/[H^+])[RNO^+]$, and eq 6 is reduced to 7,

$$-d[RNO^+]/dt = 2k_{-2}(K_5/[H^+])[H_2O_2]_o[RNO^+] \qquad (7)$$

$k_{obs} = 2k_{-2}K_5[H_2O_2]_o/[H^+]$. Using the data in Table 1 we calculated $k_{-2} = (1.4 \pm 0.2) \times 10^8$ and $(3.3 \pm 0.5) \times 10^8$ M^{-1} s^{-1} for TPO+ and 3-CP+, respectively. In the presence of sufficiently high amounts of added nitroxide the second term in the denominator of eq 6 is negligible, and eq 6 is transformed into 8:

$$-\frac{d[RNO^+]}{dt} = \frac{2k_3(K_4/[H^+])(K_5/[H^+])[H_2O_2]_o}{K_2[RNO^{\bullet}]} \times [RNO^+]^2 \qquad (8)$$

Indeed, the first-order decay of TPO+ in the presence of excess H_2O_2 at pH 4.0 turned into a second-order kinetics upon the addition of TPO, and the observed second-order rate constant decreased with the increase in [TPO]. A plot of $1/k_{obs}$ vs [TPO] was linear (Figure 4), and from the slope of the line we calculated $k_3/k_2 = 53 \pm 10$. However, the latter value varies considerably upon minor changes in the pH, for example, k_3/k_2 = 42 at pH 4.05 and 33 at pH 4.1.

Table 2. Summary of All the Rate Constants Obtained in the Present Study

	TPO/TPO⁺	3-CP/3-CP⁺
k_2, $M^{-1}s^{-1}$	$(1.2 \pm 0.1) \times 10^8$	$(1.3 \pm 0.1) \times 10^6$
k_{-2}, $M^{-1}s^{-1}$	$(1.4 \pm 0.2) \times 10^8$	$(3.3 \pm 0.5) \times 10^8$
k_3, $M^{-1}s^{-1}$	$(3.4 \pm 0.2) \times 10^9$	$(5.0 \pm 0.2) \times 10^9$
k_9, $M^{-1}s^{-1}$	(0.83 ± 0.05)	5.3 ± 0.6
k_{10}, $M^{-1}s^{-1}$	(0.48 ± 0.02)	$(7.3 \pm 0.2) \times 10^{-2}$
$E°$, V	0.75	0.89

The Reaction of the Oxoammonium Cation with Formate and CH₃OH. It had been reported that oxoammonium salts oxidize alcohols to aldehydes and ketones.[21] Since alcohols and formate are widely used in pulse radiolysis to produce superoxide, we studied their reactions with the oxoammonium cation using the stopped-flow technique. The decay of the oxoammonium cation at pH 6.9 (42 mM PB) obeyed first-order kinetics, and k_{obs} was linearly dependent on [MeOH] or [HCO₂⁻]. The decay rate at a constant [formate] decreased in acidic solutions, for example, ca. 6-fold decrease at pH 2.9 in the presence of 0.5 M formate, suggesting that the oxoammonium cation oxidizes mainly HCO_2^- ($pK_a = 3.55$ $I = 0.1-1$ M) rather than the protonated form. In addition, the reaction of 3-CP⁺ and TPO⁺ (<100 μM) with 0.45 M formate and 1 M MeOH at pH 6.9 (42 mM PB) was studied in the presence of 150 μM TNM, which reacts rapidly with both $CO_2^{\bullet-}$ and $O_2^{\bullet-}$ to form $C(NO_2)_3^-$ ($\epsilon_{350} = 14400$ M^{-1} cm^{-1}). Formation of the $C(NO_2)_3^-$ intermediate is expected, if the oxidation of formate and methanol takes place via a one-electron-transfer reaction, that is, no H-atom abstraction. However, the formation of $C(NO_2)_3^-$ was not detected at 350 nm, which indicates that the oxoammonium cations oxidize formate and alcohol through a two-electron-transfer reaction:

$$RNO^+ + HCO_2^- \rightarrow RNO\text{-}H + CO_2 \quad (9)$$

$$RNO^+ + CH_3OH \rightarrow RNO\text{-}H + H_2CO + H^+ \quad (10)$$

The rate constants for reactions 9 and 10 were calculated from the dependence of k_{obs} on methanol or formate concentrations and are compiled in Table 2.

The Reaction of the Oxoammonium Cation with NADH. The reaction of TPO⁺ and 3-CP⁺ with NADH at pH 7.0 in aerated solutions was studied by following the bleaching of NADH at 340 nm. The reaction was too fast for a kinetic study using the stopped-flow technique. The stoichiometry of the reaction was determined to be $\Delta[NADH]/\Delta[RNO^+] = 0.97 \pm 0.05$. Had NAD• been formed as an intermediate, a stoichiometry of 0.5 would have been observed because NAD• reacts rapidly with O_2 to form $O_2^{\bullet-}$. Therefore, we conclude that the oxidation of NADH by the oxoammonium cation takes place via a two-electron-transfer reaction:
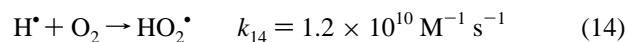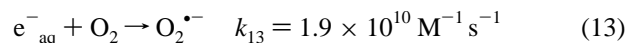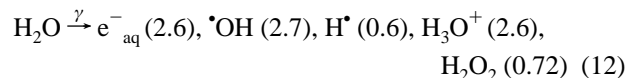
$$RNO^+ + NADH \rightarrow RNO\text{-}H + NAD^+ \quad (11)$$

This result is in agreement with earlier observations[15] where the EPR signal of the nitroxide disappeared in the presence of a flux of $O_2^{\bullet-}$ and NADH and could be restored by adding ferricyanide, which oxidizes RNO-H to the corresponding nitroxide.

(21) Bobbitt, J. M. *J. Org. Chem.* **1998**, *63*, 9367−9374.
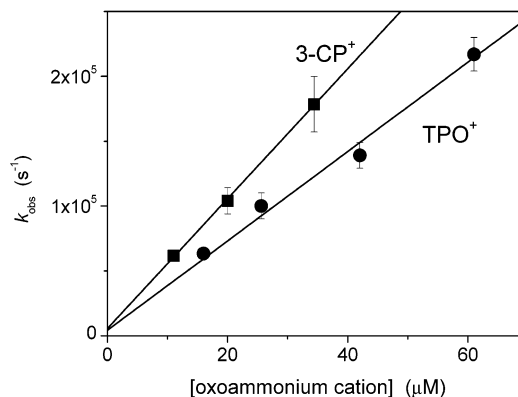
Figure 5. Reaction of oxoammonium cations with $O_2^{\bullet-}$. The decay of $O_2^{\bullet-}$ in oxygenated solutions containing 4 mM PB at pH 7.6 and various concentrations of 3-CP⁺ (■) or TPO⁺ (●) was followed spectrophotometrically. The dose was 7−13 Gy.

The Reaction of the Oxoammonium Cation with $O_2^{\bullet-}$. The reaction of $O_2^{\bullet-}$ with TPO⁺ and 3-CP⁺ was studied by pulse radiolysis of oxygenated solutions at pH 7.6 (4 mM PB). Under such conditions the following reactions take place (given in parentheses are the radiation-chemical yields of the species, defined as the number of species produced by 100 eV of energy absorbed):

$$H_2O \xrightarrow{\gamma} e^-_{aq} (2.6), {}^\bullet OH (2.7), H^\bullet (0.6), H_3O^+ (2.6),$$
$$H_2O_2 (0.72) \quad (12)$$

$$e^-_{aq} + O_2 \rightarrow O_2^{\bullet-} \quad k_{13} = 1.9 \times 10^{10} M^{-1} s^{-1} \quad (13)$$

$$H^\bullet + O_2 \rightarrow HO_2^\bullet \quad k_{14} = 1.2 \times 10^{10} M^{-1} s^{-1} \quad (14)$$

$${}^\bullet OH + RNO^+ \rightarrow products \quad (15)$$

Since the rate constant of the reaction of •OH with organic compounds is close to the diffusion-controlled limit, the rate of reaction 15 is expected to resemble that of reaction 3, and the effect of reaction 15 on the initial concentration of RNO⁺ at relatively low pulse intensity could be ignored, that is, $[O_2^{\bullet-}]_o \approx [{}^\bullet OH]_o \approx 2-4$ μM, $[RNO^+]_o > 10$ μM. The decay rate of $O_2^{\bullet-}$ at 260−280 nm was linearly dependent on $[RNO^+]$ (Figure 5), and from the slope of the lines in Figure 4 we calculated $k_3 = (5.0 \pm 0.2) \times 10^9$ and $(3.4 \pm 0.2) \times 10^9$ M^{-1} s^{-1} for 3-CP⁺ and TPO⁺, respectively.

The Reaction of the Nitroxides with $HO_2^\bullet$. The reaction kinetics of $HO_2^\bullet$ with TPO and 3-CP were studied in oxygenated solutions containing 0.01−0.15 M formate at pH < 3.7. Under such conditions all the primary radicals formed by the radiation are converted into $HO_2^\bullet$ ($\epsilon_{max}^{225 nm} = 1400$ M^{-1} cm^{-1}). Unless otherwise stated, 5 μM diethylenetriaminepentaacetc acid (DTPA) was added to avoid catalysis of superoxide dismutation by traces of metal ions.

In the presence of 100−300 μM TPO, the formation of an intermediate with a maximum absorption at 290 nm was observed, which resembles that of TPO⁺ generated electrochemically and shown in the inset of Figure 1. Typical kinetic traces at pH 3.6 are given in Figure 6. The rate of the formation obeyed first-order kinetics and was linearly dependent on [TPO] and independent of pH in range of 3.0−3.7 (Table 3). However, unlike TPO⁺ formed via electrooxidation, which was stable for 2 − 3 h, the absorption decayed within a few seconds in a first-
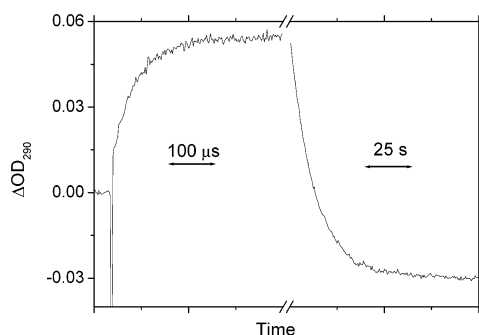
Figure 6. Formation and decay of the absorbance at 290 nm after pulse radiolysis of O$_2$-saturated solution containing 0.15 M formate and 100 μM TPO at pH 3.6. The dose was 18 Gy, and the optical path length was 12.1 cm.

Table 3. Observed Pseudo-First-Order Rate Constants (s^{-1}) for the Decay of HO$_2^\bullet$ and of RNO$^+$ as a Function of [TPO], [Formate], and pH

	[RNO], μM	[formate], mM	pH	k_{HO_2}	k_{RNO^+}
TPO	100	150	3.0	$(1.5 \pm 0.1) \times 10^4$	$(3.0 \pm 0.1) \times 10^{-2}$
TPO	150	40	3.0	$(2.1 \pm 0.2) \times 10^4$	
TPO	300	40	3.0	$(4.1 \pm 0.3) \times 10^4$	
TPO	450	40	3.0	$(5.6 \pm 1.0) \times 10^4$	
TPO	150	20	3.3	$(2.1 \pm 0.3) \times 10^4$	$(9.4 \pm 0.8) \times 10^{-3}$
TPO	100	150	3.6	$(1.5 \pm 0.1) \times 10^4$	$(7.5 \pm 0.4) \times 10^{-2}$
3-CP	75	40	2.8	206 ± 20	0.036 ± 0.004
3-CP	150	40	2.8	338 ± 52	0.033 ± 0.004
3-CP	300	40	2.8	569 ± 90	0.035 ± 0.004
3-CP	100	20	3.2	231 ± 19	0.031 ± 0.003
3-CP	200	20	3.2	397 ± 31	0.034 ± 0.003
3-CP	200	100	3.2		0.16 ± 0.01

order reaction, and the rate of the decay increased upon increasing the pH and [formate] (Table 3). A rate constant of ca. 1 M^{-1} s^{-1} was calculated for the reaction of the intermediate with HCO$_2^-$. Since the differential spectrum of TPO$^+$ has a maximum absorption at 290 nm (Figure 1, inset) and TPO$^+$ reacts with HCO$_2^-$ with a similar rate constant (Table 1), we conclude that the reaction of HO$_2^\bullet$ with TPO yields TPO$^+$ (reaction 2), and $k_2 = (1.2 \pm 0.1) \times 10^8$ M^{-1} s^{-1} (Table 3). To further examine this conclusion, the experiment was repeated in the presence of 50–300 μM ABTS^{2-} using 3.2 Gy/pulse. The yield of ABTS$^{\bullet-}$ was 74 ± 3%, and the rate of its formation was independent of [ABTS^{2-}], at pH range of 3–3.6, and linearly dependent on [TPO] (Figure 7). Hence, the rate-determining step of the formation of ABTS$^{\bullet-}$ is reaction 2, and from the slope of the line in Figure 7 we obtained $k_2 = (1.2 \pm 0.1) \times 10^8$ M^{-1} s^{-1}. When ABTS^{2-} was replaced by NADH, bleaching of NADH was observed, and Δ[NADH]/Δ[HO$_2^\bullet$] was determined to be 0.94 at pH 4.1. These results further support the occurrence of reaction 2. The kinetics of the reaction at this pH was not studied because NADH is not stable in acidic solutions.

The rate of the reaction of HO$_2^\bullet$ with 3-CP was found to be considerably slower than that with TPO. The absorption formed at 280 nm immediately after the pulse decayed via two subsequent first-order reactions. The fast decay was linearly dependent on [3-CP] (Table 3) and is attributed to the reaction of HO$_2^\bullet$ with 3-CP. The rate of the slow decay increased upon increasing the pH or [formate] (Table 3). The rate constant for the reaction of HCO$_2^-$ with the intermediate was calculated to be 5.5 ± 0.3 M^{-1} s^{-1}, which agrees with the value determined
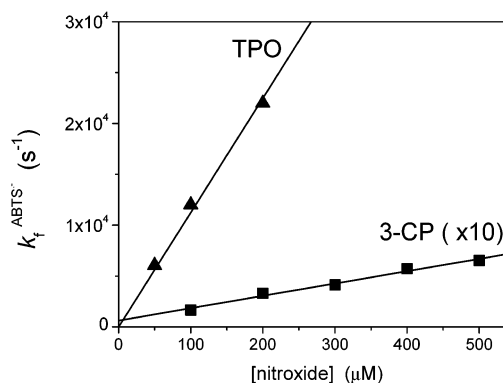
Figure 7. The reaction of nitroxides with HO$_2^\bullet$ in the presence of ABTS^{2-}. The formation of ABTS$^{\bullet-}$ was followed at 660 nm in oxygenated solutions containing 100 μM ABTS^{2-}, 20 mM formate, and (▲) TPO at pH 3.3 and (■) 3-CP at pH 3.0. The dose was 3.2 Gy.

Table 4. Bimolecular Rate Constant (M^{-1} s^{-1}) for the Reaction of Superoxide with Nitroxides as a Function of pH

pH	3-CP	TPO
4.3		7.9×10^7
4.5	1.0×10^6	
4.8	8.3×10^5	5.0×10^7
5.3		2.6×10^7
5.5	2.8×10^5	
6.1	9.7×10^4	
6.3		3.5×10^6
6.9	9.9×10^3	9.2×10^5
7.5	3.2×10^3	
7.8		1.3×10^5
8.7		1.7×10^4

^{a} The decay of superoxide was followed at 270–290 nm after pulse radiolysis of oxygenated solutions containing 10–40 mM formate, 100–600 μM nitroxide, 5 μM DTPA and 1 mM acetate or 4 mM PB.

for the reaction of 3-CP$^+$ with HCO$_2^-$, that is, k_9 (Table 2). The accumulation of 3-CP$^+$ was lower than that of TPO$^+$ since $k_3 \gg k_2$. Therefore, the reaction kinetics were studied by following the decay of HO$_2^\bullet$, and the rate constant evaluated from the data in Table 3, that is, $(1.6 \pm 0.1) \times 10^6$ M^{-1} s^{-1}, exceeds k_2. The latter value was determined in the presence of ABTS^{2-}, which competes efficiently with O$_2^{\bullet-}$ for 3-CP$^+$ at pH 3. The yield of ABTS$^{\bullet-}$ was found to be 89 ± 4%, and the rate of its formation was independent of [ABTS^{2-}] and linearly dependent on [3-CP] (Figure 7), which results in $k_2 = (1.3 \pm 0.1) \times 10^6$ M^{-1} s^{-1}. In the presence of 100 μM NADH, and at pH 4.1 we determined Δ[NADH]/Δ[HO$_2^\bullet$] $\approx$ 1.0.

Upon increasing the pH, the rate of reaction 2 decreases, and that of reaction 3 increases. Therefore, the accumulation of the oxoammonium cation decreases upon increasing the pH under limiting concentrations of superoxide. In addition, the absorption of O$_2^{\bullet-}$ ($\epsilon_{max}^{250\ nm} = 2250$ M^{-1} cm^{-1}) is greater than that of HO$_2^\bullet$, and therefore the decay of superoxide could be followed at pH > 4. The decay obeyed first-order kinetics, and k_{obs} was linearly dependent on the nitroxide concentration. The bimolecular rate constants derived from such dependence at various pHs are summarized in Table 4 and plotted in Figure 8. An excellent fit to sigmoidal curves was obtained using pK = 4.8 and assuming an asymptotic value lower than 1×10^3 M^{-1} s^{-1}.

The rates of the decay of HO$_2^\bullet$/O$_2^{\bullet-}$ under limiting concentrations of superoxide were unaffected at all pHs by the number of pulses delivered into the solution. The catalytic activity under
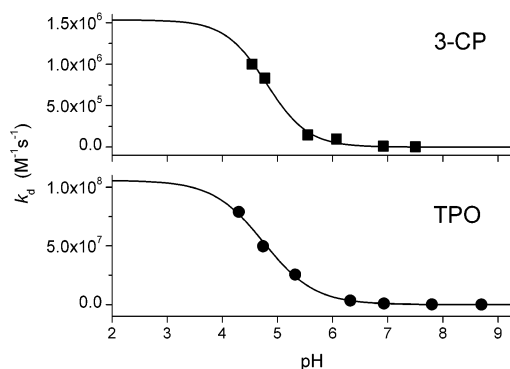
Figure 8. Decay rate constant of superoxide with TPO ($\bullet$) and 3-CP ($\blacksquare$) as a function of pH. The solid lines are sigmoidal fits to the data using pK = 4.8 and assuming that the lower asymptote values are lower than 1×10^3 M^{-1} s^{-1}. The upper asymptote values obtained through this fit are $(1.1 \pm 0.1) \times 10^8$ and $(1.5 \pm 0.1) \times 10^6$ M^{-1} s^{-1} for TPO and 3-CP, respectively.
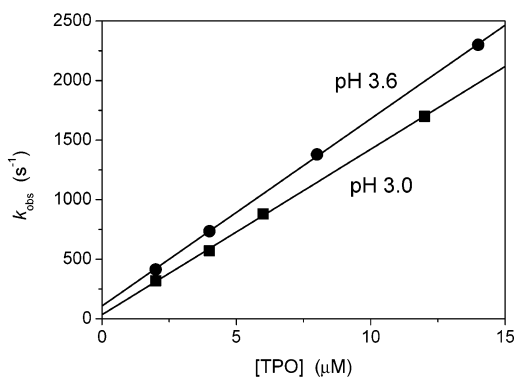

Figure 9. TPO-catalyzed dismutation of superoxide. The decay of 22 μM $HO_2^{\bullet}$ generated upon pulse radiolysis of oxygenated solutions containing TPO, 10 mM formate and 5 μM DTPA at pH 3.0 ($\blacksquare$) and 3.5 ($\bullet$) was followed at 260 nm.

limiting concentration of the nitroxide can be studied using the pulse radiolysis only under conditions where the catalytic rate exceeds that of the spontaneous dismutation of superoxide. In the present case this condition is met for TPO but not for 3-CP and only in acidic solutions. Thus, the decay of 22 μM $HO_2^{\bullet}$ in the presence of 2–14 μM TPO was followed at 255–260 nm and found to obey first-order kinetics. The observed first-order rate constant was linearly dependent on [TPO] (Figure 9), which results in $k_{cat} = 1.4 \times 10^8$ and 1.6×10^8 M^{-1} s^{-1} at pH 3.0 and 3.5, respectively.

Discussion

The present study demonstrates that TPO and 3-CP catalyze the dismutation of superoxide by utilizing the $RNO^{\bullet}/RNO^+$ redox couple. The oxoammonium cation is formed in the reaction of $HO_2^{\bullet}$ with the nitroxide, and the rate constant for the reaction of $O_2^{\bullet-}$ with the nitroxide is at least 3 orders of magnitude lower. The difference of about 2 orders of magnitude between the values of k_2 for TPO and 3-CP is related to the difference between the redox potentials of the $RNO^{\bullet}/RNO^+$ couples. The redox potentials have been calculated using the data in Table 2, that is, $K_2 = 0.86 \pm 0.22$ and $(3.9 \pm 1.4) \times 10^{-3}$ for TPO and 3-CP, respectively. Since $\Delta E_2^{\circ} = (RT/nF)$ $\ln K_2$ and $\Delta E_2^{\circ} = E^{\circ}(HO_2^{\bullet}/HO_2^-) - E^{\circ}(RNO^+/RNO^{\bullet})$, we used $E^{\circ}(HO_2^{\bullet}/HO_2^-) = 0.75$ V[22] and calculated $E^{\circ}(TPO^+/TPO) =$

(22) Stanbury, D. M. *Adv. Inorg. Chem.* **1989**, *33*, 69–138.
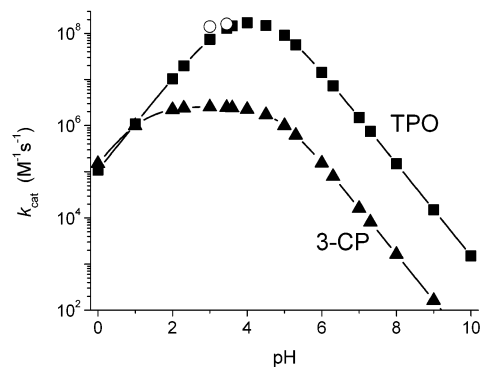
Figure 10. Calculated pH dependence of the catalytic rate constant of superoxide dismutation by nitroxides. The data points were calculated using eq 19 and the rate constants given in Table 2. The open symbols are experimental values.

0.75 V and $E^{\circ}(3\text{-}CP^+/3\text{-}CP) = 0.89$ V. These values are in good agreement with the midpoint redox potentials 0.74 and 0.87 V, respectively, previously determined using cyclic voltammetry.[18]

Assuming that reaction 2 takes place via an outer-sphere electron-transfer mechanism, we can use the Marcus equation $k_{12} = (k_{11}k_{22}K_{12}f_{12})^{1/2}$ to calculate k_2. Here k_{12} is the electron-transfer rate constant for the cross reaction, k_{11} and k_{22} are the self-exchange rate constants for the reactants, K_{12} is the cross reaction equilibrium constant, and $\ln f_{12} = (\ln K_{12})^2/[4 \ln(k_{11}k_{22}/10^{22})]$.[23] Since the self-exchange rate constant for $HO_2^{\bullet}/HO_2^-$ has been determined to be 17 M^{-1} s^{-1},[24] and that for $RNO^{\bullet}/RNO^+$ cannot exceed 1×10^{10} M^{-1} s^{-1}, we calculated $k_2 < 3.8 \times 10^5$ M^{-1} s^{-1} for TPO and $< 2.6 \times 10^4$ M^{-1} s^{-1} for 3-CP. These calculated values are orders of magnitude lower than the experimental values, and therefore reaction 2 must take place via an inner-sphere electron-transfer mechanism:

$$RNO^{\bullet} + HO_2^{\bullet} \rightleftharpoons \text{adduct} \quad (16)$$

$$\text{adduct} \rightarrow RNO^+ + HO_2^- \quad (17)$$
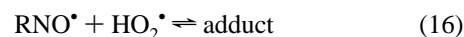
Thus, $k_2 = k_{16}k_{17}/(k_{-16} + k_{17})$, and assuming that k_{16} is diffusion-controlled, k_{-16}/k_{17} should be ca. 10^2 for TPO and ca. 10^4 for 3-CP. It is also likely that reaction 17 is both [H^+]- and general acid-catalyzed, for example, according to reaction 18,

$$\text{adduct} + H^+ \rightarrow RNO^+ + H_2O_2 \quad (18)$$
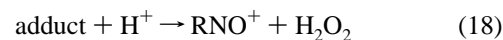
and perhaps k_2 increases at very high [H^+] for both nitroxides.

Reactions 2 and 3 are pH-dependent, and assuming the steady-state approximation for the oxoammonium cation, one obtains rate eq 19 under limiting concentrations of superoxide, where $([O_2^{\bullet-}] + [HO_2^{\bullet}]) = [O_2^{\bullet-}]_T$, and $([RNO^{\bullet}] + [RNO^+]) = [RNO^{\bullet}]_o$:

$$-\frac{d[O_2^{\bullet-}]_T}{dt} = \frac{2k_2k_3}{(1 + [H^+]/K_4)k_2 + (1 + K_4/[H^+])k_3} \times$$
$$[RNO^{\bullet}]_o[O_2^{\bullet-}]_T = k_{cat}[RNO^{\bullet}]_o[O_2^{\bullet-}]_T \quad (19)$$

The simulated curves for k_{cat} vs pH for TPO and 3-CP are plotted in Figure 10. The dependence of k_{cat} on the pH displayed

(23) Marcus, R. A. *J. Phys. Chem.* **1963**, *67*, 853–857.
(24) Lind, J.; Shen, X.; Merenyi, G.; Jonsson, B. O. *J. Am. Chem. Soc.* **1989**, *111*, 7654–7655.

bell-shaped curves having a maximum around pH 4 and demonstrates that the catalytic activity of the nitroxides under physiological conditions predominantly depends on k_2. For instance, with low fluxes of $O_2^{\bullet-}$, for example, 1 μM/min, TPO at 3 μM is sufficient to decrease the steady-state concentration of $O_2^{\bullet-}$ at pH 7.4 by ca. 95%, whereas 250 μM 3-CP is required to achieve the same effect.

Conclusions

The oxoammonium cation is a one-electron oxidant of $ABTS^{2-}$, ferrocyanide, and HO_2^-, whereas the oxidation of methanol, formate, and NADH occurs through a two-electron-transfer reaction. The diverse biological antioxidant behavior of nitroxides can be attributed in part to the $RNO^{\bullet}/RNO^+$ couple, that is, SOD activity. In addition, in many cases the one-electron oxidation yields toxic intermediates, and therefore the ability of the oxoammonium cation to accept two electrons can contribute to the antioxidant activity of the nitroxides. However, the oxoammonium cation is also a strong one-electron oxidant, which may lead to adverse biological effects. The search for more effective nitroxide SOD-mimics should concentrate on those having lower redox potential for the couple $RNO^{\bullet}/RNO^+$, that is, higher values for the oxidation rate of the nitroxide by $HO_2^{\bullet}$, and maximal k_{cat} at pHs closer to physiological pH. In the present study the effect of charge and lipophilicity were not examined, although they are important in targeting nitroxides into selective subcellular sites.